Computerized Analysis of Lesions in US Images of the Breast[1]

Maryellen L. Giger, PhD, Hania Al-Hallaq, BS, Zhimin Huo, PhD, Catherine Moran, BA
Dulcy E. Wolverton, MD, Chun Wai Chan, MS, Weiming Zhong, MS

Rationale and Objectives. Breast sonography is not routinely used to distinguish benign from malignant solid masses because of considerable overlap in their sonographic appearances. The purpose of this study was to investigate the computerized analyses of breast lesions in ultrasonographic (US) images in order to ultimately aid in the task of discriminating between malignant and benign lesions.

Materials and Methods. Features related to lesion margin, shape, homogeneity (texture), and posterior acoustic attenuation pattern in US images of the breast were extracted and calculated. The study database contained 184 digitized US images from 58 patients with 78 lesions. Benign lesions were confirmed at biopsy or cyst aspiration or with image interpretation alone; malignant lesions were confirmed at biopsy. Performance of the various individual features and output from linear discriminant analysis in distinguishing benign from malignant lesions was studied by using receiver operating characteristic (ROC) analysis.

Results. At ROC analysis, the feature characterizing the margin yielded A_z values (area under the ROC curve) of 0.85 and 0.75 in distinguishing between benign and malignant lesions for the entire database and for an "equivocal" database, respectively. The equivocal database contained lesions that had been proved to be benign or malignant at cyst aspiration or biopsy. Linear discriminant analysis round-robin runs yielded A_z values of 0.94 and 0.87 in distinguishing benign from malignant lesions for the entire database and for the equivocal database, respectively.

Conclusion. Computerized analysis of US images has the potential to increase the specificity of breast sonography.

Key Words. Artificial intelligence; breast imaging; computer-aided diagnosis; computer vision; differential diagnosis; US imaging.

Breast cancer is a leading cause of death in women, causing an estimated 44,000 deaths per year (1). Mammography is the most effective method for early detection of breast cancer, and periodic screening of asymptomatic women reduces the mortality rate (2–4). Many breast cancers are detected, and these patients are referred for biopsy on the basis of a radiographically observed mass lesion or cluster of microcalcifications. General rules for the differentiation of benign from malignant mammographically identified breast lesions exist (5,6), but considerable misclassification of these lesions still occurs. On average, less than 30% of masses referred for surgical breast biopsy are actually malignant (7).

Breast sonography is an important adjunct to diagnostic mammography, and it is typically performed on palpable and/or mammographically identified masses to determine their cystic or solid nature. The accuracy rate of ultrasonography (US) has been reported to be 96%–100% in the diagnosis of simple benign cysts (8), and masses so characterized do not require further evaluation. US has not been used for screening purposes, however, because of relatively high false-negative and false-positive rates. Even so, US is being evaluated as a potential screening method in women with dense breasts (9). Physicians at

Acad Radiol 1999; 6:665–674

[1] From the Department of Radiology, MC 2026, Kurt Rossmann Laboratories for Radiologic Image Research, University of Chicago, 5841 S Maryland Ave, Chicago, IL 60637. Received December 31, 1998; revision requested February 2, 1999; revision received June 10; accepted June 15. Supported in part by National Institutes of Health grant P20 CA66132 and U.S. Army Medical Research and Materiel Command grant DAMD17-98-1-8194. **Address reprint requests to** M.L.G.

M.L.G. is a shareholder in R2 Technology, Inc (Los Altos, Calif). It is the University of Chicago Conflict of Interest Policy that investigators disclose publicly actual or potential significant financial interest that would reasonably appear to be directly and significantly affected by the research activities.

some centers are successful at visually distinguishing benign from malignant masses by using US, but physicians at most facilities are unable to rely on breast US to avoid biopsy because of the considerable overlap in the sonographic appearances of these masses.

With the advent of modern, high-frequency transducers that have improved spatial and contrast resolution, however, several sonographic features have emerged as potential indicators of malignancy and others as potential indicators of benign masses (10,11). Benign features include hyperechogenicity, ellipsoid shape, mild lobulation, and a thin, echogenic pseudocapsule. Malignant features include spiculation, angular margins, marked hypoechogenicity, posterior acoustic shadowing, and a depth-to-width ratio greater than 0.8.

Stavros et al (12) used various features to characterize masses as being either benign, indeterminate, or malignant. Their classification scheme had a sensitivity of 98.4% and a negative predictive value of 99.5%. The sonographic evaluation described by these investigators, however, is much more extensive and complex than that usually performed at most breast-imaging centers. US is a notoriously operator-dependent modality, and until these encouraging results are corroborated through additional studies by other investigators, it is unclear how widely applicable or reliable such sonographic classification schemes truly are.

Computer-aided techniques have been applied to color Doppler US evaluation of breast masses with promising results (13). Color Doppler imaging is a technique that focuses on the vascularity of lesions. Not all sonographically visible cancers have demonstrable neovascularity, however, and benign lesions can be vascular. Therefore, the sensitivity and specificity of this technique are inherently somewhat limited. These limitations have been demonstrated in power Doppler imaging of solid breast masses (14).

Comprehensive summaries of investigations regarding mammographic computer-aided diagnosis have been published (15,16). During the 1960s and 1970s, several investigators attempted to analyze mammographic abnormalities by using computers (17–24). These investigators demonstrated the potential capability of computers in the detection of mammographic abnormalities. Gale et al (17) and Getty et al (18) both reported on computer-based classifiers that take diagnostically relevant features obtained from radiologists' readings of breast images as input. Getty et al found that with use of this classifier, community radiologists performed as well as unaided expert mammographers in differentiating benign from malignant lesions. In addition, Swett and Miller (19) developed an expert system to provide both visual and cognitive feedback to radiologists by using a critiquing approach combined with an expert system. At the University of Chicago, we have shown that computerized analysis of mass lesions (21,23) and clustered microcalcifications (22,24) as shown on digitized mammograms yields performance rates similar to those of expert mammographers and significantly better ($P < .05$) than those of average radiologists in distinguishing malignant from benign lesions.

US is a digital modality that is amenable to application of computer-aided diagnosis techniques that could ultimately be used in a real-time fashion (at the time of examination) to improve diagnostic accuracy. Given that sonographic interpretation is a subjective process, however, and that criteria have been developed that may allow for differentiation of benign from malignant solid breast masses, it is reasonable to assume that computer-aided diagnosis techniques applied to sonographic images would also improve radiologists' performance, particularly when this method is combined with corresponding mammographic data (25). Recently, Garra et al (26) showed promising results with the use of computer-extracted features derived from co-occurrence matrices of images of breast lesions.

In this study, we attempted to determine if computer analysis of breast lesions in gray-scale, US images could be used to discriminate malignant from benign lesions.

MATERIALS AND METHODS

Database

Masses were viewed sonographically by filming representative images in orthogonal planes. The US examinations were performed with an Ultramark 9 with High Definition Imaging (HDI) from Advanced Technology Laboratories (Bothell, Wash) with a high-frequency, 7.5-MHz, electronically focused, near-field imaging probe. The static images of lesions that did not contain overlaid cursors or color Doppler signals were used in this study.

The US film images were retrospectively collected and then digitized with a laser film scanner (KFDR-S; Konica, Tokyo, Japan) with a scanner pixel size of 0.1 mm and 10-bit quantization. Each multiformat film contained only one US image. Film digitization is not the optimal approach to acquiring digital US data, but it was the only one available for this initial study.

The 58 patients in the study ranged in age from 35 to 89 years (mean age, 53 years). They had 78 masses as shown on 184 digitized US images. Benign lesions were confirmed at biopsy or cyst aspiration or with image interpretation alone, whereas malignant lesions were confirmed at biopsy. Of the total 184 images, 144 were from 43 patients with 62 benign lesions, and 40 were from 15 patients with 16 malignant lesions. Benign lesions included simple cysts, complex cysts, and solid masses. Of the 62 benign lesions, 19 (all solid) were proved at biopsy, five (1 solid lesion and four complex cysts) were proved at cyst aspiration, and 38 (four solid lesions and 34 cysts) were deemed to be benign on the basis of visual interpretation of the US images alone. All 16 malignant lesions were proved at biopsy.

Lesions were further subcategorized into an "equivocal" category on the basis of the necessity of performing an interventional procedure to determine their status. The 24 benign lesions that were proved at biopsy or cyst aspiration and the 16 malignant lesions made up the equivocal database (total, 40 lesions). The purpose of this subcategorization was to determine the ability of the computer features to distinguish benign from malignant lesions that required an interventional procedure (cyst aspiration or biopsy) for definitive diagnosis.

Manual Lesion Segmentation and Region-of-Interest Selection

Once digitized, the US images were displayed on an IBM monitor, and a breast-imaging radiologist (D.E.W.) outlined the approximate margins of each lesion. Figure 1 shows US images of breast lesions with outlined margins. Regions of interest (ROIs) of 32 × 32 pixels were selected from regions within and around the lesions. Features were calculated on the basis of the manually extracted lesion margin or the 32 × 32-pixel ROI.

Automated Feature Extraction

Four types of lesion characteristics were investigated: margin, shape, homogeneity (texture), and posterior acoustic attenuation. Table 1 lists these characteristics and their relationships to benign and malignant lesions.

The lesion characteristics were quantified by using various computer-extracted features, and Table 2 lists the computer-extracted features used in distinguishing malignant from benign lesions. Features were calculated either along or within the lesion margin or within the 32 × 32-pixel ROI (placed within the central portion of or posterior to the lesion).

To quantify the lesion margin characteristics, a gradient analysis was performed along a computer-expanded margin of the lesion. In this analysis, the manually extracted margin was first expanded by using morphologic filtering. Next, this region was processed by using a Sobel filter to obtain the gradient and its direction at each pixel. The normalized radial gradient was then calculated to quantify the margin sharpness and degree of irregularity (shape) (21,27). The normalized radial gradient (21,27) is given by the equation

$$\text{normalized radial gradient} = \frac{\sum_{P \in \text{margin}} \cos\varphi \sqrt{D_x^2 + D_y^2}}{\sum_{P \in \text{margin}} \sqrt{D_x^2 + D_y^2}},$$

where D_x is the gradient along the x axis, D_y is the gradient along the y axis, and φ is the angle between the gradient vector and the radial gradient. A lower value for the normalized radial gradient indicates a less distinct margin.

The geometric measure of shape in terms of a short-to-long axis ratio for each lesion was determined by using the image data along the margin. Note here that the short-to-long axis ratio corresponds to a depth-to-width ratio to extract the orientation of the long axis. Cysts tend to be ellipsoid, thereby resulting in a depth-to-width ratio of much less than 1, whereas malignant lesions tend to have a vertical or round axial orientation (28).

Texture can be described through spatial relationships between image pixels by using changes in the intensity patterns and gray levels. Texture characteristics of the homogeneity within the lesion were determined by using a measure of coarseness (29). The texture measure of coarseness (local uniformity) is given by the equation

$$\text{coarseness} = \left[\sum_{i}^{G_h} p_i s(i)\right]^{-1},$$

where G_h is the highest gray-level value in the ROI and p_i is the probability of occurrence for gray level i. Thus, if N is the width of the ROI ($N = 32$), d is the neighboring size (half the operating kernel size W), the ith entry of s is given by

$$s(i) = \begin{cases} \sum |i - A_i| & \text{for } i \in \{N_i\} \text{ if } N_i \neq 0 \\ 0 & \text{otherwise} \end{cases}$$

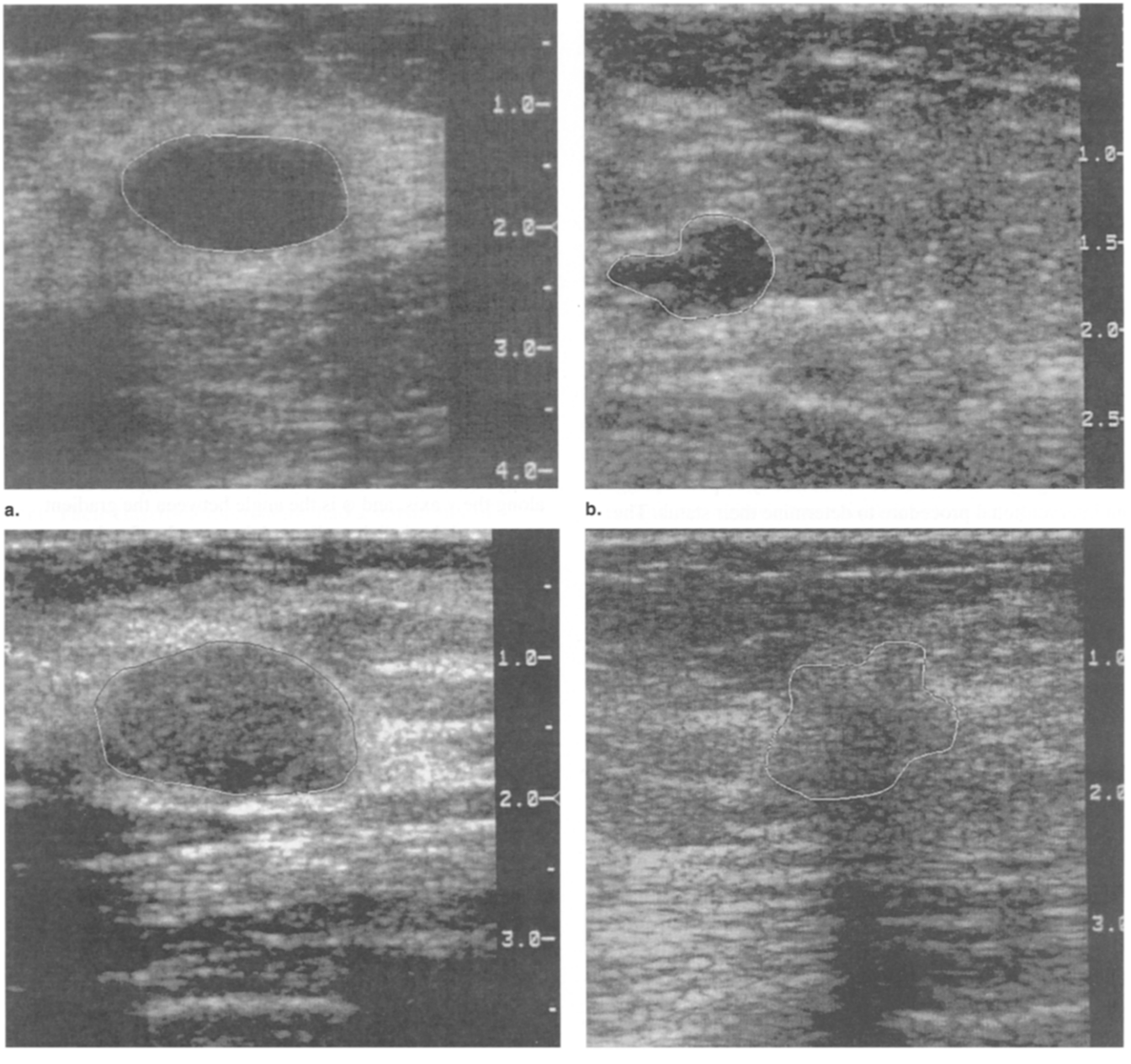

Figure 1. **(a)** US image of a simple cyst. **(b)** US image of a complex cyst. **(c)** US image of a benign solid lesion. **(d)** US image of a malignant lesion, along with radiologist-drawn lesion margin.

where $\{N_i\}$ is the set of pixels having gray level i,

$$A_i = \frac{1}{W-1} \sum_{p=-d}^{d} \sum_{p=-d}^{d} f(x+p, y+q)$$

$$(p, q) \neq (0,0) \text{ to exclude } (x, y)$$

$$W = (2d+1)^2 \qquad (d = 3).$$

Thus, a lower value of coarseness corresponds to a finer visual texture.

The computerized assessment of posterior acoustic attenuation or enhancement associated with different lesions was determined in two ways: (*a*) by comparing the gray-level values within the lesion with those posterior to that lesion and (*b*) by comparing the gray-level values posterior to the lesion with those in adjacent tissue at the same depth. These calculations were performed to quantify

Table 1
Lesion Characteristics and Their Relationship to Benign and Malignant Lesions

Characteristic	Benign (Cystic or Solid)	Malignant
Lesion margin	Smooth borders	Angular margins, spiculation
Lesion shape	Ellipsoid, mildly lobulated	Irregular; depth-to-width ratio, >0.8
Texture within lesion	Anechoic, hyperechoic, reverberation artifacts	Hypoechoic
Posterior acoustic attenuation	Posterior enhancement	Posterior shadowing

the amount of any posterior acoustic shadowing or enhancement. For example, benign lesions are often associated with posterior enhancement, whereas malignant lesions are often associated with posterior shadowing. Simple cysts that are anechoic produce less attenuation of the US waves than surrounding parenchyma produces and, thereby, cause relative hyperechogenicity posterior to the lesion. In this analysis, 32 × 32-pixel ROIs were placed within the lesion, posterior to the lesion, and in the adjacent tissue at the same depth, and the differences in average gray levels were then calculated to quantify the posterior acoustic attenuation.

The feature value for a given lesion was obtained by averaging that feature value over all views of the lesion. Each lesion had from two to five images available from one clinical examination.

Linear discriminant analysis (LDA) was used to merge the four individual, computer-extracted features into a single index related to an estimate for the likelihood of malignancy. In LDA, the discriminant function is formulated by using a linear combination of the individual features (30). Both consistency and round-robin runs were performed. In round-robin analysis, the discriminant function is trained on all but one case and is then tested on that remaining case; this process is repeated until all cases have been individually tested.

Evaluation

Receiver operating characteristic (ROC) analysis (31) was used to evaluate (by case, not by image) the performance of the individual computer-extracted features in distinguishing benign from malignant lesions. The decision variable for the ROC analysis was each individual feature. The area under the ROC curve (A_z) was used as an indicator of performance. Specificity at high sensitivity is relevant clinically, because the cost of missing a cancer is greater than the cost of performing an interventional procedure for a benign lesion. Therefore, we also calculated the performance of the features in the high-sensitivity range (true-positive fraction [TPF_0], >0.90) by using the partial area index ($_{TPF_0}A_z'$), which is the portion of the area under the ROC curve that lies above the true-positive fraction divided by the constant (1 – TPF_0) (32). Both A_z and partial A_z values were calculated for the entire database and for the equivocal database.

RESULTS

The A_z values for the various computer-extracted US features ranged from 0.54 to 0.85 in distinguishing benign from malignant lesions. Table 2 provides these values for both the entire database and the equivocal database. Because missing a cancer is more important clinically than performing an interventional procedure for a benign lesion, we used the partial area index to quantify performance of the features at a high-sensitivity level (32). Table 2 provides these $_{TPF_0}A_z'$ values for the entire database and the equivocal database.

When the first four features (listed in Table 2) were used, LDA consistency runs yielded A_z values of 0.95 and 0.93 in distinguishing benign from malignant lesions for the entire database and the equivocal database, respectively, and the round-robin runs yielded A_z values of 0.94 and 0.87 in distinguishing benign from malignant lesions for the entire database and the equivocal database, respectively (Table 2). When the second posterior acoustic attenuation feature was used, LDA consistency runs yielded A_z values of 0.94 and 0.93 in distinguishing benign from malignant lesions for the entire database and the equivocal database, respectively, and the round-robin runs yielded A_z values of 0.92 and 0.86 in distinguishing benign from malignant lesions for the entire database and the equivocal database, respectively (Table 2).

DISCUSSION

Figure 2 shows cluster plots of the coarseness and margin features for malignant and benign lesions in the entire database and the equivocal database. Figure 3 shows clus-

Table 2
Computer-extracted Features Used to Quantify Lesion Characteristics

Analysis	Region for Database	Entire Database*		Equivocal Database†	
		A_z	$_{0.90}A_z$	A_z	$_{0.90}A_z$
Lesion margin					
1. Normalized radial gradient	Margin	0.85	0.46	0.75	0.28
Shape					
2. Depth-to-width ratio	Margin	0.67	0.20	0.75	0.29
Texture within the lesion					
3. Coarseness	ROI	0.54	0.12	0.67	0.14
Posterior acoustic attentuation					
4. Difference in gray level between "within lesion" and posterior to lesion	ROIs	0.77	0.29	0.72	0.27
5. Difference in gray level between "posterior to lesion" and adjacent tissue at same depth	ROIs	0.83	0.35	0.72	0.17
Linear discriminant analysis (features 1, 2, 3, and 4)					
Consistency analysis		0.95	0.78	0.93	0.70
Round-robin analysis		0.94	0.76	0.87	0.56
Linear discriminant analysis (features 1, 2, 3, and 5)					
Consistency analysis		0.94	0.68	0.93	0.58
Round-robin analysis		0.92	0.59	0.86	0.38

Note.—Performance is given in terms of A_z and partial A_z for the entire database and the "equivocal" database in distinguishing malignant from benign lesions.
*n = 78 cases.
†n = 40 cases.

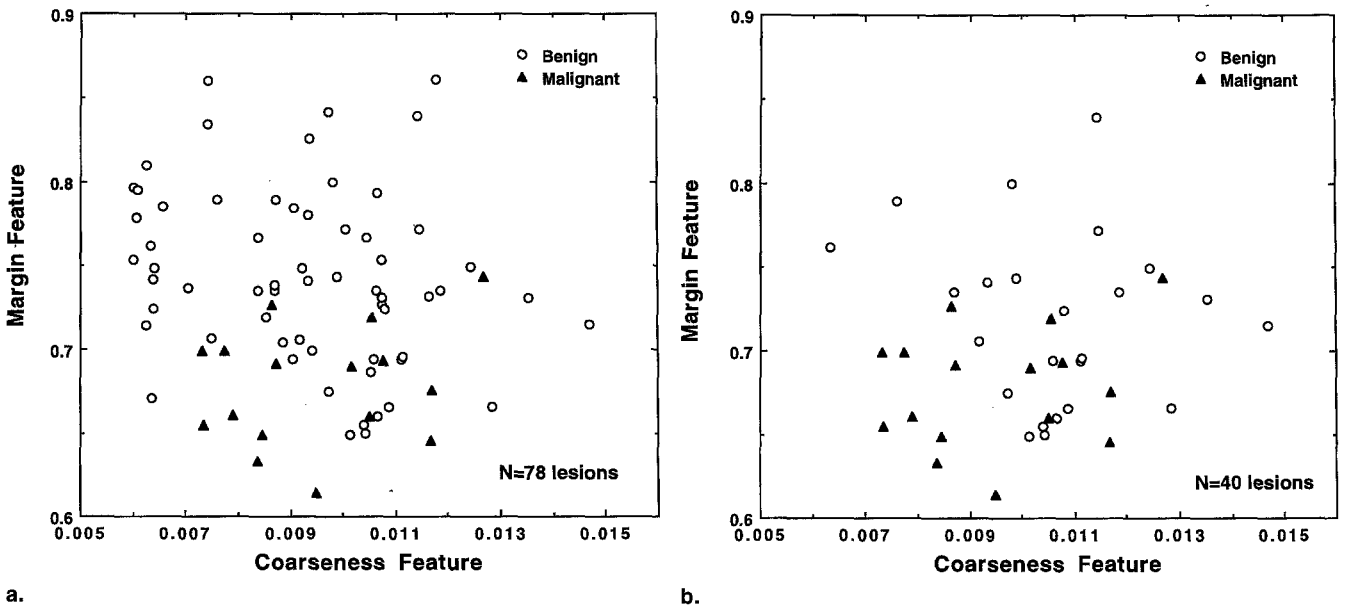

Figure 2. Cluster plots indicate feature values for margin and texture. **(a)** Values for the entire database. **(b)** Values for the equivocal database.

ter plots of the depth-to-width ratio and the (first) posterior acoustic attenuation feature for malignant and benign lesions in the entire database and the equivocal database. As these figures show, malignant lesions tend to exhibit less distinct margins and more posterior shadowing than benign lesions as documented by using visual US criterion (10,12,26,28). It is interesting that many benign lesions not in the equivocal database of this study had a very

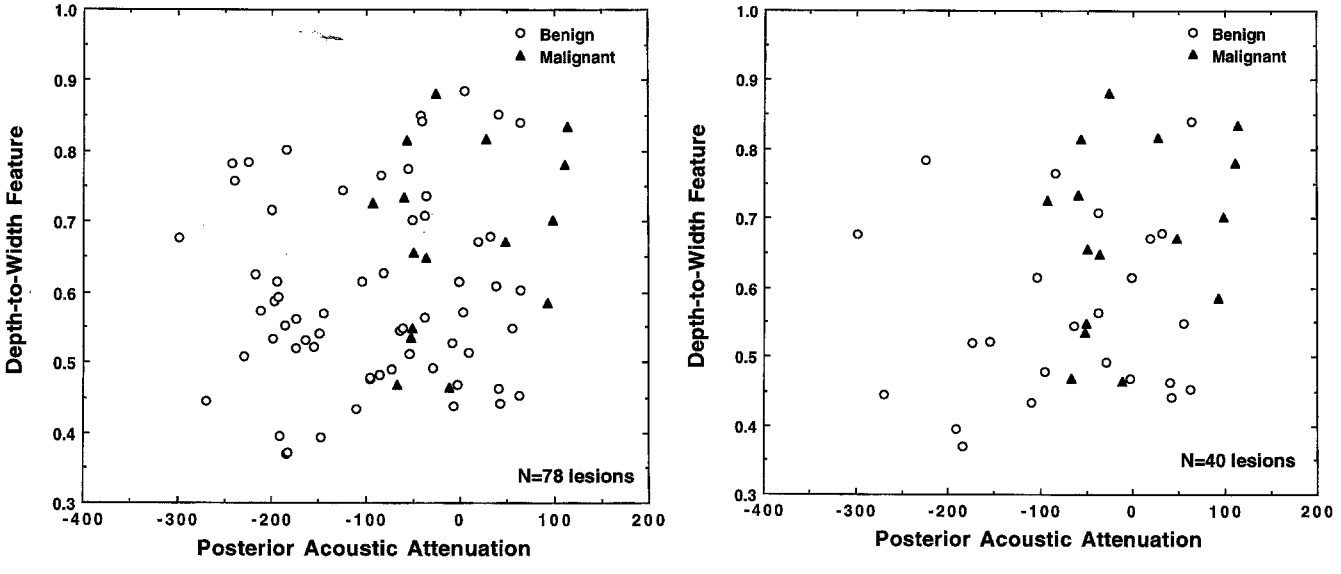

Figure 3. Cluster plots indicate feature values for lesion shape and posterior acoustic attenuation. **(a)** Values for the entire database. **(b)** Values for the equivocal database.

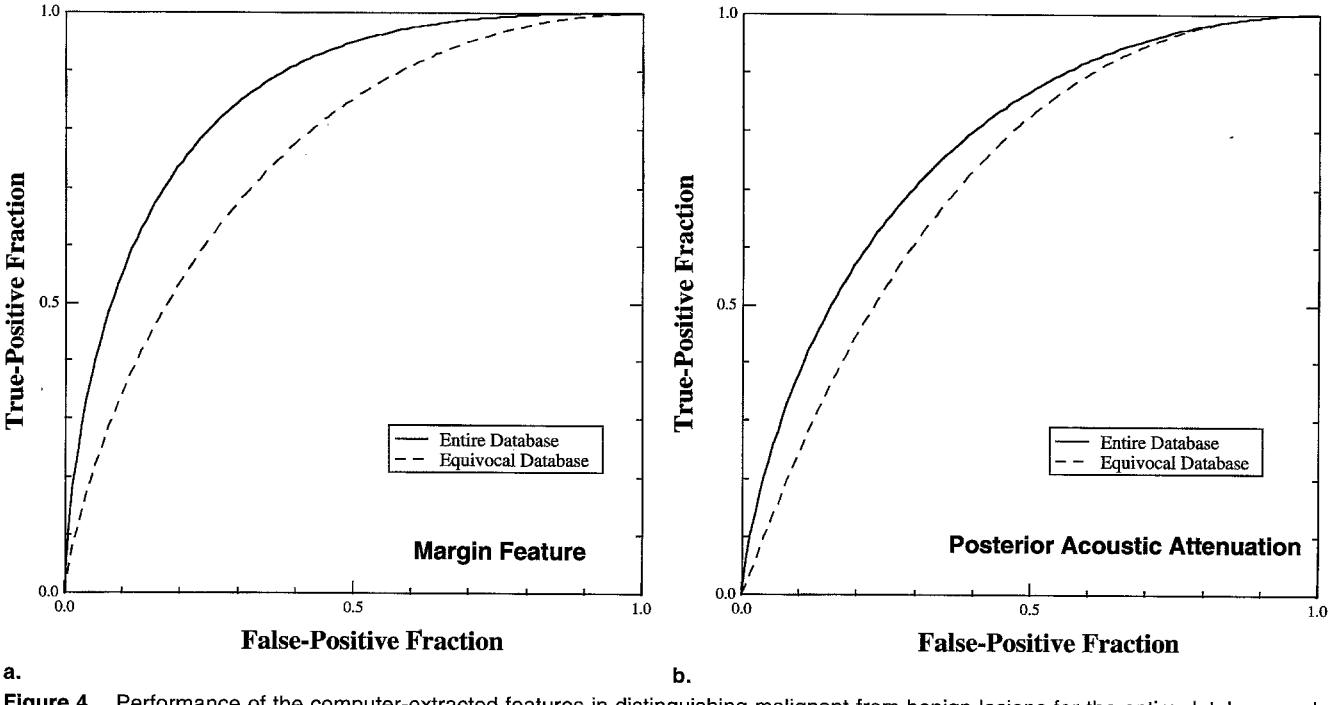

Figure 4. Performance of the computer-extracted features in distinguishing malignant from benign lesions for the entire database and for the equivocal database. **(a)** Margin. **(b)** Posterior acoustic attenuation.

"fine" texture (a low coarseness feature), because many were cysts and anechoic. In contrast, the benign solid lesions tended to have a coarse texture.

Figure 4 shows performance in terms of ROC curves for the features characterizing margin and acoustic attenuation in distinguishing malignant from benign lesions for the entire database and for the equivocal database. The ROC curves are lower for the equivocal database than for the entire database, thereby indicating that as for radiologists, benign lesions in the equivocal database are more difficult to distinguish from malignant lesions. Figure 5, which shows histograms of the feature values (for malig-

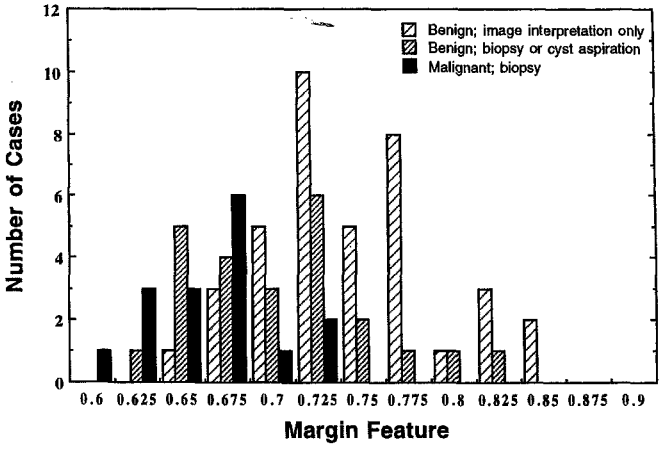

a.

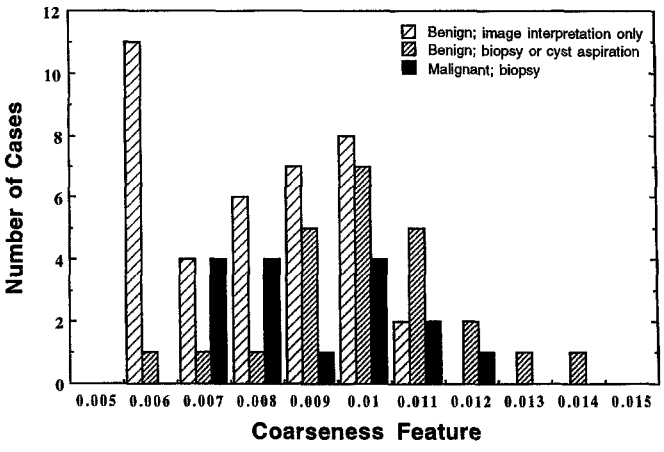

b.

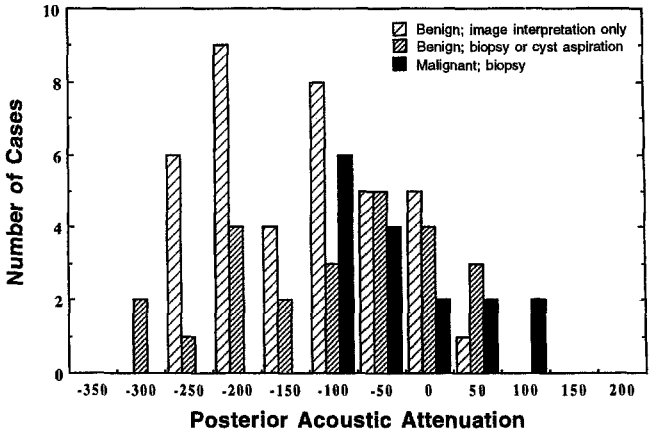

c.

Figure 5. Histograms of the computer-extracted features of the benign nonequivocal database, benign equivocal database, and malignant database. **(a)** Margin. **(b)** Texture. **(c)** Posterior acoustic attenuation.

nant lesions, benign lesions in the equivocal database, and the remaining benign lesions) for margin, texture, and posterior acoustic attenuation, further illustrates this point. As shown, malignant lesions tend to exhibit a coarse texture, less distinct margins, and posterior shadowing. There is, however, substantial overlap in the features of malignant and features of benign lesions in the equivocal database.

Table 2 and Figure 6 show perfomance of the linear discriminant function in distinguishing malignant from benign lesions for the entire database and the equivocal database. Of note are the partial A_z values and the shape of the ROC curves. Extraction from the fitted ROC curves for the equivocal database (in which all lesions underwent a clinical procedure [cyst aspiration or biopsy]) indicates that at a high sensitivity level (90%) for malignant cases, 30% of the benign cases were classified as benign and, thus, could potentially have avoided biopsy. Therefore, combined use of the four computer-extracted features yields superior performance.

Film digitization was not the optimal approach to acquiring our digital US database, but it was the only one available for this study. Even with the limited image quality obtained from digitization of the multiformat film US images, however, we could observe computer features capable of distinguishing malignant from benign lesions. Computerized analysis of direct digital US data is expected to improve the discriminatory value of the various features, especially for texture features of the lesion interior. Our future database collection will include direct digital data.

The purpose of this study was to determine if computer-extracted features on US images of breast lesions have the potential to discriminate malignant from benign lesions and, thus, ultimately help to reduce the number of unnecessary biopsies performed. This potential has been shown even though the number of lesions in the database is small. In addition, the features chosen for this study agree well with those used by radiologists when interpreting breast US images. It should be noted, however, that the computer-extracted features were obtained from radiologist-drawn margins. In the future, the subjectiveness of human-drawn margins will be eliminated with use of computer segmentation.

US images of the breast can yield information on the interior of the lesion (homogeneity), as well as on the interface of the lesion with its surroundings. This is why US is used to distinguish solid from cystic lesions. Gradient analysis of the margin yields information on the lesion margin, including its sharpness and shape. Geometric features relating to the depth-to-width ratio of the lesion are also useful, because even though many solid lesions may be ellipsoid, the orientation of the ellipse regarding the

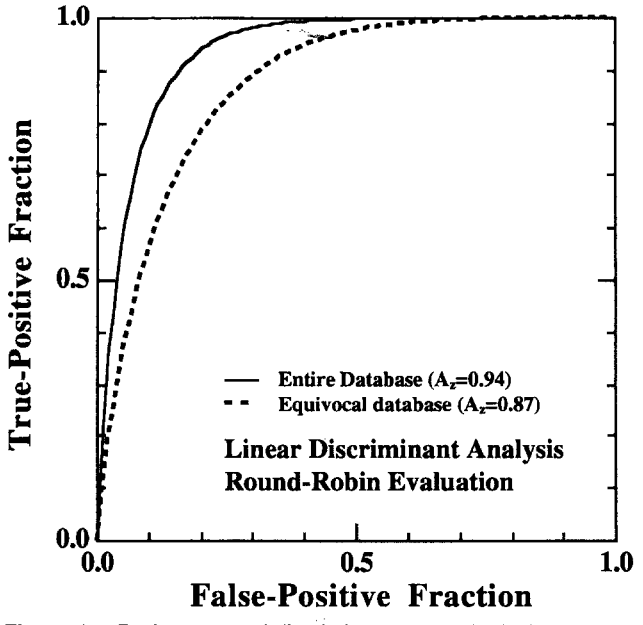

Figure 6. Performance of discriminant scores in distinguishing malignant from benign lesions for the entire database and the equivocal database. Results are from round-robin analyses.

skin is important in distinguishing benign from malignant lesions. In addition, computerized analysis allows for an objective assessment of posterior acoustic shadowing and enhancement, which can also aid in distinguishing benign from malignant lesions. It should be noted, however, that because shadowing depends on gain settings, scanning parameters should be set more automatically than they are at present.

Use of LDA as a classifier with which to merge the four computer-extracted features was useful for improving performance in distinguishing malignant from benign lesions for both the entire database and the equivocal database. As the overall database increases, other classifiers such as artificial neural networks will be investigated as means with which to merge these features into an estimate of the likelihood of malignancy.

In conclusion, we have developed methods for the computer analysis of breast lesions in US images. In this study, we automatically extracted and calculated features related to lesion margin, shape, texture (homogeneity) within the lesion, and posterior acoustic attenuation. From ROC analyses of the computer-extracted features, the features based on margin characteristics yielded A_z values of 0.85 and 0.75 in distinguishing benign from malignant lesions for the entire database and the equivocal database, respectively. The equivocal database consisted of lesions that had been proved to be benign or malignant at either cyst aspiration or biopsy. LDA consistency runs yielded A_z values of 0.95 and 0.93 in distinguishing benign from malignant lesions for the entire database and the equivocal database, respectively, and the round-robin runs yielded A_z values of 0.94 and 0.87 in distinguishing benign from malignant lesions for the entire database and the equivocal database, respectively. Our results indicate that computerized analysis of US images has the potential to increase the specificity of breast sonography. These promising results warrant further development and testing on a large, direct-digital database.

ACKNOWLEDGMENTS

The authors thank Fred Winsberg, MD, for contributing to the database and Ulrich Bick, MD, Jason Rubenstein, Michael Chinander, and Samuel Armato III, PhD, for useful discussions.

REFERENCES

1. American Cancer Society. Cancer facts and figures—1998. New York, NY: American Cancer Society, 1998.
2. Feig SA. Decreased breast cancer mortality through mammographic screening: results of clinical trials. Radiology 1988; 167:659–665.
3. Tabar L, Fagerberg G, Duffy SW, Day NE, Gad A, Grontoft O. Update of the Swedish two-county program of mammographic screening for breast cancer. Radiol Clin North Am 1992; 30:187–210.
4. Smart CR, Hendrick RE, Rutledge JH, Smith RA. Benefit of mammography screening in women ages 40 to 49 years: current evidence from randomized controlled trials. Cancer 1995; 75:1619–1626.
5. Bassett LW, Jackson VP, Jahan R, Yao SF, Gold RH. Diagnosis of diseases of the breast. Philadelphia, Pa: Saunders, 1997.
6. Kopans DB. Breast imaging. Philadelphia, Pa: Lippincott, 1998.
7. Brown ML, Houn F, Sickles EA, Kessler LG. Screening mammography in community practice: positive predictive value of abnormal findings and yield of follow-up diagnostic procedures. AJR 1995; 165:1373–1377.
8. Jackson VP. The role of US in breast imaging. Radiology 1990; 177: 305–311.
9. Kolb TM, Lichy J, Newhouse JH. Occult cancer in women with dense breasts: detection with screening US—diagnostic yield and tumor characteristics. Radiology 1998; 207:191–199.
10. Tohno E, Cosgrove DO, Sloane JP. Ultrasound diagnosis of breast diseases. Edinburgh, Scotland: Churchill Livingstone, 1994; 50–73.
11. Fornage BD, Lorigan JG, Andry E. Fibroadenoma of the breast: sonographic appearance. Radiology 1989; 172:671–675.
12. Stavros AT, Thickman D, Rapp CL, Dennis MA, Parker SH, Sisney GA. Solid breast nodules: use of sonography to distinguish between benign and malignant lesions. Radiology 1995; 196:123–134.
13. Huber S, Delorme S, Knopp MV, et al. Breast tumors: computer-assisted quantitative assessment with color Doppler US. Radiology 1994; 192:797–801.
14. Birdwell RL, Ikeda DM, Jeffrey SS, Jeffrey RB Jr. Preliminary experience with power Doppler imaging of solid breast masses. AJR 1997; 169:703–707.
15. Giger ML. Computer-aided diagnosis. In: Haus A, Yaffe M, eds. Syllabus: a categorical course on the technical aspects of breast imaging. 2nd ed. Oak Brook, Ill: Radiological Society of North America, 1993; 272–298.
16. Vyborny CJ, Giger ML. Computer vision and artificial intelligence in mammography. AJR 1994; 162:699–708.
17. Gale AG, Roebuck EJ, Riley P, et al. Computer aids to mammographic diagnosis. Br J Radiol 1987; 60:887–891.
18. Getty DJ, Pickett RM, D'Orsi CJ, Swets JA. Enhanced interpretation of

diagnostic images. Invest Radiol 1988; 23:240–252.
19. Swett HA, Miller PA. ICON: a computer-based approach to differential diagnosis in radiology. Radiology 1987; 163:555–558.
20. Giger ML, Vyborny CJ, Schmidt RA. Computerized characterization of mammographic masses: analysis of spiculation. Cancer Lett 1994; 77: 201–211.
21. Huo Z, Giger ML, Vyborny CJ, et al. Analysis of spiculation in the computerized classification of mammographic masses. Med Phys 1995; 22: 1569–1579.
22. Jiang Y, Nishikawa RM, Wolverton DE, et al. Automated feature analysis and classification of malignant and benign clustered microcalcifications. Radiology 1996; 198:671–678.
23. Huo Z, Giger ML, Vyborny CJ, Wolverton DE, Schmidt RA, Doi K. Automated computerized classification of malignant and benign mass lesions on digitized mammograms. Acad Radiol 1998; 5:155–168.
24. Jiang Y, Nishikawa RM, Schmidt RA, Metz CE, Giger ML, Doi K. Improving breast cancer diagnosis with computer-aided diagnosis. Acad Radiol 1999; 6:22–33.
25. Giger ML, Huo Z, Wolverton DE, et al. Computer-aided diagnosis of digital mammographic and ultrasound images of breast mass lesions. In: Karssemeijer N, Thijssen M, Hendriks J, van Erning L, eds. Digital mammography 1998. Dordrecht, the Netherlands: Kluwer, 1998; 143–147.
26. Garra BS, Krasner BH, Horii SC, Ascher S, Mun SK, Zeman RK. Improving the distinction between benign and malignant breast lesions: the value of sonographic texture analysis. Ultrason Imaging 1993; 15: 267–285.
27. Bick U, Giger ML, Schmidt RA, Doi K. A new single-image method for computer-aided detection of small mammographic masses. In: Lemke HU, Inamura K, Jaffe CC, Vannier MW, eds. Proceedings of CAR '95. 1995; 357–363.
28. Sohn C, Blohmer JU, Hamper UM. Breast ultrasound: a systematic approach to technique and image interpretation. New York, NY: Thieme, 1998.
29. Amadasun M, King R. Textural features corresponding to textural properties. IEEE Trans Syst Man Cybern 1989; 19:1264–1274.
30. Lachenbruch PL. Discriminant analysis. London, England: Hafner, 1975.
31. Metz CE. Some practical issues of experimental design and data analysis in radiological ROC studies. Invest Radiol 1989; 24:234–245.
32. Jiang Y, Metz CE, Nishikawa RM. A receiver operating characteristics partial area index for highly sensitive diagnostic tests. Radiology 1996; 201:745–750.